Back to Papers

Chaotic and Other Oscillations of Pipelines

J D Fenton
Professor, Dept. of Civil Engineering, University of Auckland, Auckland, NZ

A C Josem
Research Fellow, Dept. of Mechanical Engineering, Monash University, Clayton, Australia

J B Hinwood
Associate Professor, Dept. of Mechanical Engineering, Monash University, Clayton, Australia

SUMMARY This paper studies the nonlinear dynamics of pipes subject to ocean waves and currents. It examines the nature of the oscillations of pipelines subject to fluctuating loading by both an experimental study and a theoretical and computational study. The experiments provide a view of the remarkable complexity of the problem, while the other study attempts to describe the effects of individual terms in the governing equations, and how the various terms affect the nature of pipe oscillations. The paper is descriptive, concentrating on trying to understand the processes at work.

1. INTRODUCTION

The motion of an elastically-mounted cylinder has been observed in an oscillating water column. For small-amplitude fluid oscillations, the motion of the cylinder was a regular small-amplitude transverse oscillation. As the fluid oscillations were increased, the motion of the cylinder became a wild, erratic, and possibly chaotic motion. This has raised the question as to whether or not the motion was actually chaotic in nature.

An overview of chaotic systems is given in Parker and Chua (1989), and there are many modern presentations of a more-or-less popular nature. There are four main types of steady-state behaviour of a dynamical system. In order of increasing complexity they are equilibrium, periodic solutions such as a limit cycle, quasi-periodic solutions *(i.e.* expressible as a countable sum of periodic functions), and finally chaos. There is no widely accepted definition of chaos. It can be defined as "none of the previous cases", such that for practical purposes, it is bounded steady-state behaviour that is not at an equilibrium point, not periodic, and not quasi-periodic.

Chaotic trajectories are attracted to a *strange attractor,* an object in state space with complicated properties. Well-known examples are those which appear in solutions of the Lorenz equations. One characteristic of most chaotic systems is that they show *sensitive dependence on initial conditions,* so that given two sets of initial conditions of a dynamical system, arbitrarily close to one another, the trajectories emanating from these initial conditions diverge until they become uncorrelated. This is the situation of the so-called "Butterfly Effect" whereby the equations of meteorology show that the beating of a butterfly's wings could subsequently alter the state of the weather halfway across the world. Practically, this means that there is a limit to the predictability of the weather, even though the equations can be solved numerically.

It is well-known that the periodically forced motion of a nonlinear oscillator can exhibit chaotic motions. For example, Bryant and Miles (1990) considered the motion of a pendulum to which a periodically-varying torque is applied. The equation of motion is

$$\ddot{x} + c\dot{x} + \sin x = F \sin \omega t , \qquad (1)$$

where x is the angular displacement from the downward vertical, each dot denotes differentiation with respect to time t, c is a damping coefficient, F is a measure of the torque applied, which in the scaled variables used here, is applied at a frequency ω times the natural frequency. The equation is nonlinear, because the dependent variable x appears as the argument of a trigonometric function. In this situation, the motions show a high degree of chaos, depending on the magnitude of the forcing. If the amplitudes of oscillation are small, then $\sin x$ in equation (1) can be replaced to good approximation by x, the equation is linear, and solutions show simple harmonic motion at the natural frequency of the pendulum plus a further harmonic motion at the forcing frequency ω. There is no chaos.

2. ONE-DIMENSIONAL OSCILLATIONS OF A BODY SUBJECT TO OSCILLATING FLOW

2.1 Elastic restraint

The relevance of the model equation (1) to the subject of this paper is suggested by the equation governing the motion of bodies subject to fluid velocity fields, namely Newton's second law of motion, where the force is given by the empirical Morison equation. The one dimensional form of the resulting equation is:

$$(M+\rho(C_m-1)V)\ddot{x} + C\dot{x} + Kx =$$
$$\rho V C_m \dot{u}(t) + \frac{\rho}{2} C_d A \, (u(t)-\dot{x}) \, |u(t)-\dot{x}| \, , \quad (2)$$

where

M = mass of the body,
ρ = fluid density,
C_m = inertia coefficient,
V = volume of the body,
x = *linear* displacement of the body,
C = structural damping coefficient,
K = stiffness of the elastic system,
C_d = drag coefficient of the fluid on the body,
A = area of the body transverse to the flow,
$u(t)$ = fluid velocity.

The broad similarity between this second-order differential equation and equation (1) becomes clear on detailed comparison. This equation does not contain a nonlinear restoring force (it has Kx instead of $\sin x$), but it does contain a nonlinear term due to the drag force of the fluid on the body, where there is a term which varies like $\dot{x}$ multiplied by a term which includes $\dot{x}$ and which can abruptly change gradient as the relative velocity changes sign.

Initially we examined solutions of this equation for various combinations of parameters. No unusual behaviour at all was found. It is interesting to gain an insight into the reason for that and the expected nature of solutions by considering the nature of the equation. Dividing through by the coefficient of the second derivative gives:

$$\ddot{x} + C'\dot{x} + K'x = C'_m \dot{u}(t) + C'_d \, (u(t)-\dot{x}) \, |u(t)-\dot{x}| , \quad (3)$$

where the definitions of the coefficients shown with primes can be easily obtained by performing the elementary operations.

It is convenient to rewrite the equation in a pseudo-linear form by writing the magnitude of the fluid velocity relative to the body as $u_r(t) = |u(t)-\dot{x}|$, and re-arranging to give

$$\ddot{x} + (C' + C'_d u_r(t))\,\dot{x} + K'x = C'_m \dot{u}(t) + C'_d \, u_r(t)\, u(t) \, . (4)$$

In this form, similarities to equation (1) or to the equation for any linear oscillator become clear. The role of the fluid drag is now more obvious. On the left side of the equation it appears with the structural damping. Hence, even though the term is nonlinear, its role is to damp out the body motion. On the right side of the equation, the terms combine to act in a similar way to the case in equation (1) where the body is in a periodically-fluctuating velocity field due to waves. Both $u(t)$ and $\dot{u}(t)$ contain harmonic variation of the same wavelength. It is possible to linearly combine the two such that the net effect is an input of the same wavelength but with a different phase. A further nonlinear effect is caused by $u_r(t)$ being a discontinuous function, whose gradient changes when the fluid velocity passes the body velocity.

In the general maritime case, the right hand side illustrates a sometimes-forgotten danger which can have important repercussions for the fatigue strength of a structural member. If the input wave signal is not just a single sinusoid, but can be decomposed into a Fourier series containing a number of harmonic terms, the nonlinearity of the last term means that more harmonic terms may be present than expected - for example, even if $u(t)$ just contained a single term in $\sin \omega t$, then the nonlinearity means that terms like the square of this will be present, and an elementary trigonometric identity shows that this appears as a term in $\cos 2\omega t$ plus a constant term. In this way, the nonlinear drag term can generate higher and lower frequency components.

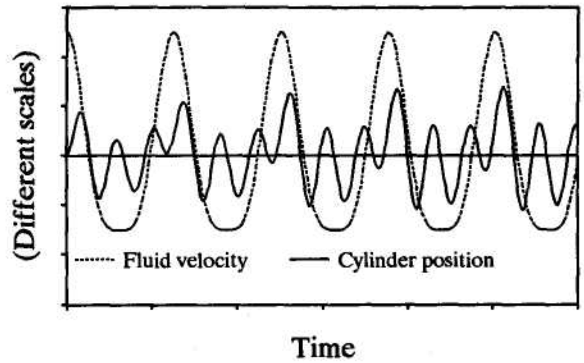

Figure 1: Incident fluid velocity and resulting motion of cylinder where oscillations at the natural frequency are excited by harmonics from the nonlinear drag term.

A more important feature is, however, that these or any other terms in the input wave signal may be close to the natural frequency of the system, which can easily be shown to be $\sqrt{K'}$ in the notation of equation (4). As an example, consider the results shown in Figure 1. The incident wave has two components, the fundamental, and one of twice the frequency but half the amplitude, leading to the marked asymmetry shown, and by its sharper crests and longer troughs mimicking the behaviour of real waves. Calculations were performed for a system whose natural frequency of oscillation was three times that of the fundamental input frequency. The figure shows that the nonlinear drag term can combine the first and second harmonics to produce a third harmonic, at the resonant frequency of the body, and the resultant output shows a very marked oscillation at this higher frequency, generally in phase with the input signal, but looking nothing like it. As the graph shows, the displacement and hence the stress in the system shows reversals at the higher frequency, giving implications for the fatigue strength. In a practical situation of course, higher harmonics than the third might be excited.

The results of this section, and all others in this paper, were obtained using the fourth-order Runge-Kutta method for solving differential equations numerically.

2.2 Nonlinear restraint

The problem may also be rendered nonlinear if the nature of the elastic restraint changes for larger deflections. An example of this in ocean engineering is the case of an articulated mooring tower driven by steady waves. This may be considered as a single degree-of-freedom oscillator whose dynamics are nonlinear by virtue of a stiffness discontinuity. The stiffness has different magnitudes for positive and negative deflections when a mooring cable tightens for positive deflection but provides no extra restraint for negative deflection. This is described in Thompson and Stewart (1986), who showed the existence of subharmonic resonances and multiple solutions depending on the starting conditions.

The effects of such a nonlinear restraint were examined in the present work, and the one-dimensional motion of a cylinder under waves was simulated, with a marked stiffness discontinuity for large deflection. Results are as shown in Figure 2. It can be seen that when the increased stiffness is encountered while the fluid holds the cylinder at an extreme position, higher frequency oscillations are set up, as might be expected based on linear considerations (frequency proportional to the square root of the stiffness), but then when the cylinder is swept in the other direction, the general oscillation corresponds to the more flexible restraint. The motion is complicated, but it is periodic and is not chaotic. Below we will see that this is not the case in two dimensions.

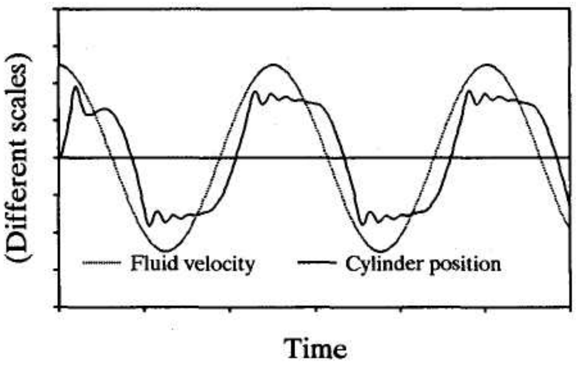

Figure 2. Complicated periodic motion with nonlinear stiffness

An additional way in which equation (4) becomes nonlinear is because the coefficients C_m and C_d in equation (2) depend on the local fluid velocity, so that coefficients in (2) will depend on $u_r(t)$. This behaviour may give rise to galloping or other large-amplitude oscillations. To test this, computations were carried out simulating the variation of the coefficient in this way, but the behaviour of the solutions were hardly affected and certainly no chaotic behaviour was noted.

To conclude this section, it can be stated that the nonlinearities in the equation governing one-dimensional oscillations gave no hint of chaotic motion.

3. EXPERIMENTS

3.1 Apparatus

The experimental facility described in Reid and Hinwood (1987) has some features which endow it with unusually-ideal conditions for the testing of a cylinder subject to oscillating flows. The apparatus shown in Figure 3 consists of a vertical U-Tube in which the water is excited to a resonant oscillation by a loose fitting plunger. This simulates the action of a wave past the cylinder which is elastically supported and weighted so that it is neutrally buoyant. It was 0.5m long, 25.4mm in diameter, had a mass of 0.25kg, and was fitted with end plates. A current can be superimposed on the oscillating flow and is controlled by a pump which circulates flow through the working section and is returned *via* a pipe. The current speeds range from 0.07 to 0.26 m/s.

The idealising features alluded to above include: (1) that the flow is parallel to the sides of the tube and there are no vertical velocities superimposed thus eliminating that extra variable, and (2) that the fluid velocities in the tube are simple harmonic, containing only a single sine wave. This is unusual in a system oscillating under gravity. For example, the pendulum described in equation (1) is a highly nonlinear system, because the restoring force is proportional to the sine of the displacement.

3.2 Observations

For small fluid velocities, the motion of the cylinder was predominantly vertical, oscillating in a direction transverse to the flow. This shows that the drag coefficient must be varying little, while the lift forces are varying appreciably due to the vortices separating from the cylinder. This is in keeping with other studies (see Chandler and Hinwood, 1985, for example).

As fluid velocities were increased, the behaviour depended very much on whether or not oscillating velocity or mean current was dominant, and provided a fascinating illustration of the different modes of behaviour possible. It was really only after traces of the path of the cylinder were recorded and plotted that the nature of the behaviour in each case became apparent. Consider the motion where there was no net current, so that the fluid velocity was that of simple harmonic motion with an amplitude of 0.12 m/s, as shown in Figure 4. A preferred type of motion is apparent, that describing something of a butterfly, but within that it can be seen that the motions are very irregular indeed. Although the shape of the butterfly was not obvious in early visual observations, the apparently-chaotic nature of the motions was, and suggested a program of further study and comparison with computer simulations.

With the addition of a current, the motions changed dramatically. Figure 5 shows some of the different and fascinating behaviour as the current was increased, while the peak wave velocity was held constant at

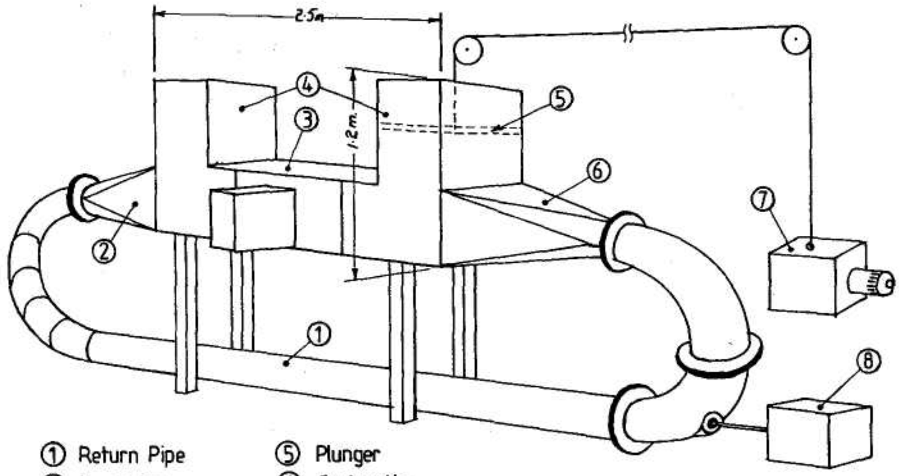

Figure 3. Experimental arrangement of the U-Tube

0.09 m/s and a frequency of 0.44Hz. Part (a) shows a complex but remarkably regular pattern. As the velocity was increased, a more random trace within a defined region became apparent, as shown by (b). At a current of 0.15 m/s the cylinder spent more time tracing a slow path in the central area, as well as making random excursions in other directions. Here the motion seemed to be chaotic. As the flow velocity was increased to 0.17 m/s, the cylinder traversed a clearly defined path avoiding the central region! The richness of the behaviour sets a considerable challenge to describe analytically and computationally.

Figure 4. Apparently chaotic motion for no current.

To conclude this section, there is ample evidence for irregular motions of an elastically-mounted cylinder in an oscillating flow. Particularly for the case of no current there seemed to be little underlying order. Whether the motions are chaotic or not was tested by computer simulation, as will now be described.

4. TWO-DIMENSIONAL OSCILLATIONS OF A BODY SUBJECT TO OSCILLATING FLOW

It is well known that systems with more degrees of freedom have a greater tendency to exhibit chaos. An example is that of the Lorenz equations for the motion of a particle, which show chaotic behaviour in three dimensions but not in two. It might be expected then, that the irregular motions observed experimentally might be able to be simulated numerically.

In two dimensions, Newton's law and the Morison equation for two dimensions yield:

$$(M+\rho(C_m-1)V)\ddot{x} + C\dot{x} + Kx = \rho V C_m \dot{u} + \frac{\rho}{2} C_d A\,(u(t)-\dot{x})\,\sqrt{(u(t)-\dot{x})^2+\dot{y}^2} + D(t), \qquad (5)$$

for the x direction (parallel to the flow), and

$$(M+\rho(C_m-1)V)\ddot{y} + C\dot{y} + Ky = \frac{\rho}{2} C_d A\,(-\dot{y})\,\sqrt{(u(t)-\dot{x})^2+\dot{y}^2} + L(t), \qquad (6)$$

for the y direction. The fluid velocity imposed in the U-tube has only a horizontal component and only a single harmonic as discussed above: $u(t) = A_0 + A_1 \cos \sigma t$, where σ is the frequency of the input wave, and A_0 is the mean current.

These equations contain extra terms $D(t)$ and $L(t)$ which are drag and lift force terms due to vortex separation. It is known (Chandler and Hinwood, 1985) that the lift term dominates and that vortex forces cannot be calculated simply in terms of drag and lift coefficients. Also, the nature of the dominant lift force is a quite complicated function of time, even for the case where the cylinder is fixed. In the present case of a compliant cylinder the details of the vortex forces must be very complicated. Here we adopt a simple approach of representing them by relatively short Fourier series:

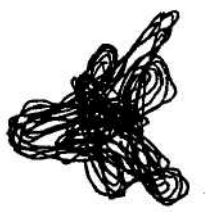

(a) Current 0.11 m/s

(b) Current 0.14 m/s

(c) Current 0.15 m/s

(d) Current 0.17 m/s

Figure 5. Changing motions of the cylinder as current increased

$$D(t) = \sum_{j} D_j e^{ij\sigma_v t} \tag{7.1}$$

$$L(t) = \sum_{j} L_j e^{ij\sigma_v t} \tag{7.2}$$

where $i = \sqrt{-1}$, the sums are usually from -3 to +3, and σ_v is the vortex shedding frequency, which in the case of lock-in will be equal to σ, the wave frequency.

Initially for the case of no current, numerical experiments were conducted with two and three-term series for the lift and drag. It was found relatively easy to simulate the results obtained by Sumer *et al.* (1989) for the path of a pipe above a scour trench. Typical results are shown in Figure 6. The Lissajous-type figures correspond to different relative magnitudes of Fourier coefficients of the lift and drag forces. The usual situation was that the lift force had a fundamental frequency twice that of the incident wave, as reported by Chandler and Hinwood (1985) and Justesen (1989). Where the fundamental lift frequency was three times the incident, reported by Justesen as a common case, a Lissajous figure similar to the logo of the Australian Broadcasting Corporation was obtained. This type of behaviour was not reported in any of our experiments or those of Sumer *et al.* (1989), who found some irregularity in their results around these basic sorts of figures, however, there was no tendency in our calculations for chaotic motions to appear.

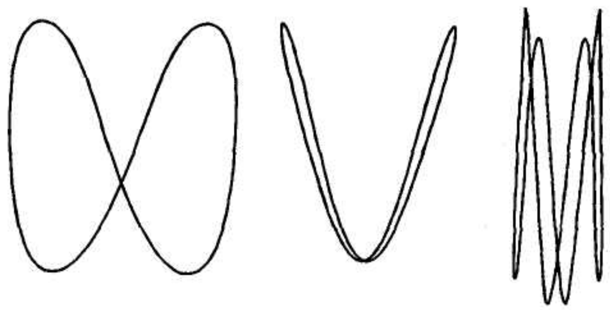

Figure 6. Pipe trajectories.

It was considered rather more important to be able to simulate the trajectories obtained in the experimental program described, as we knew the experimental parameters. For the case of no current, as shown in Figure 4, with a high degree of chaotic motion, only ordered motions were able to be simulated. Figure 7 shows something of the nature of the solutions: two trajectories are shown, each with a different set of initial conditions shown by the small rectangles. It seems, that for finite drag forces, the equations are such that the solutions approach a limit cycle, which would seem to act against the development of chaos.

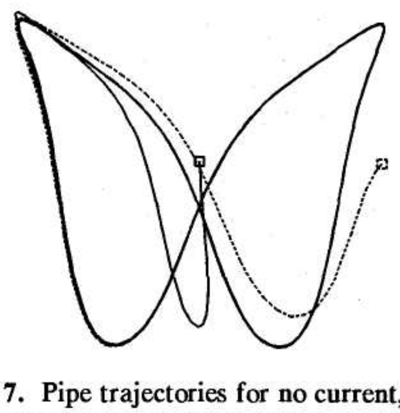

Figure 7. Pipe trajectories for no current, showing results for two different initial conditions

For the case with a current of 0.17 m/s, from Figure 5(d), the simulation is shown in Figure 8. The apparent non-uniqueness of the orbit is not a characteristic of the equations, but due to the artifice of allowing the vortex-shedding frequency to vary randomly throughout the simulation. A similar picture to the experimental one is obtained. However, there was no tendency to chaotic motion.

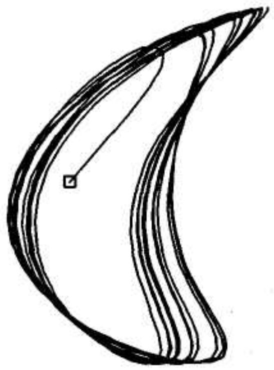

Figure 8. Pipe trajectory for a current of 0.17 m/s.

In the course of performing the computations many interesting figures and behaviours were revealed. A noteworthy one is that shown in Figure 9, for the rather idealised case of zero drag. It is included here to illuminate the effect of the drag forces in the other figures. In this case a dramatic two-periodic solution is obtained, and the solution performs often-severe contortions to remain within the envelope defined by the many osculations. It is notable that with C_d set to zero, the equations are linear, yet here show a rather more interesting behaviour.

Figure 9. Trajectories for zero drag case

To this stage of the computations, no chaotic motions have been revealed. Figure 10 shows the results of a two-dimensional computation for the bilinear stiffness case described in its one-dimensional form in #2, and pictured in Figure 2. It can be plausibly deduced that the motion is indeed chaotic. The two trajectories are for slightly different initial conditions, and it is quite clear that the two seem to have nothing to do with each other after the motion has been well-developed. The passage of the trajectory is quite dramatic, occasionally oscillating vigorously across the domain, occasionally lingering near the centre, and occasionally making great circular sweeps around the domain.

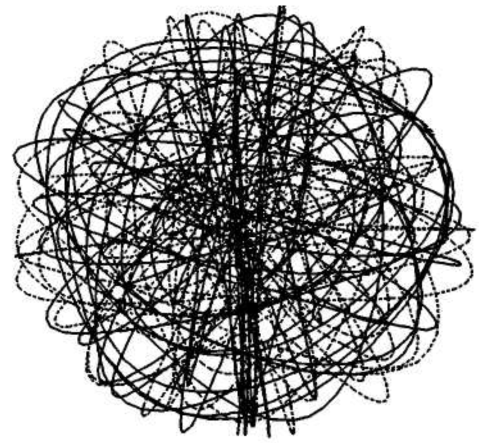

Figure 10. Chaotic motions for bilinear stiffness

5. CONCLUSIONS

We have performed experiments which show considerable complexity of behaviour, moving out of and back into chaotic regimes twice as the current was increased. Some of the features of the motion have been simulated computationally, but we have found chaotic motions only for the case of a bilinear stiffness law. Despite its strong nonlinearities in the drag term, the Morison equation seems to be one which leads naturally to limit cycle types of solutions. The drag term in the equation acts so as to conform motion to the externally applied velocity field. Any motions not conforming are quickly damped out, leading to a limit cycle of a stable periodic oscillation.

6. REFERENCES

Bryant, P.J. and J.W. Miles (1990) On a periodically forced, weakly damped pendulum. Part 1: Applied torque. /. *Austral. Math. Soc. Ser. B* 32, 1-22.

Chandler, B.D. & J.B. Hinwood (1985) Wave-induced vortex forces on horizontal cylinders. *Proc. 7th Australasian Conf. Coastal & Ocean Engnrng.*, Christchurch, N.Z., 2-6 Dec, Vol.2, 203-212.

Justesen, P. (1989) Hydrodynamic forces on large cylinders in oscillatory flow. *J. Waterway Port Coastal and Ocean Engrng.* 115, 497-514.

Parker, T.S. and L.O. Chua (1989) *Practical numerical algorithms for chaotic systems.* Springer, New York.

Reid, D.L. & J. B. Hinwood (1987) An experimental rig for study of fluid/structure interaction between elastic cylinders and ocean flows. *Proc. 8th Australasian Conf. Coastal & Ocean Engnrng.*, Launceston, 30 Nov-4 Dec, 231-234.

Sumer, B.M., J0rgen Fredsffe, H. Gravesen and R. Bruschi (1989) Response of marine pipelines in scour trenches. *J.Waterway Port Coastal and Ocean Engrng.* 115, 477-496.

Thompson, J.M.T. & H.B. Stewart (1986) *Nonlinear dynamics and chaos.* Wiley, Chichester.